W Boson Production at the Large Hadron Collider

Candidacy Paper

by

Dugan O'Neil
University of Victoria

December 1, 1997

Abstract

An examination of the importance of W production at LHC has been performed. Rates for several different production mechanisms were calculated and it was determined that single W production via Drell-Yan is the dominant production mode for high energy hadron colliders. Each LHC experiment can be expected to produce approximately 1.8×10^8 W per day at design energy and luminosity. In light of these high production rates, the usefulness of each W source and the difficulties it can cause have also been discussed.

Contents

1 Introduction

The Large Hadron Collider (LHC) will be the highest energy particle collider in the world producing proton-proton collisions at a centre of mass energy of 14 TeV. The high energy and luminosity of LHC will produce a variety of interesting physics signals. The detection and analysis of these signals will take place at two general purpose experiments, ATLAS[1] and CMS[2].

At the high centre of mass energy of LHC, very heavy mass states can be produced and the decays of many of these states will involve the production of one or more W bosons. Alternatively, many interesting signals will have backgrounds that involve W. Therefore, understanding W production at the LHC is an important issue for detecting signals and understanding backgrounds. Of course, using the LHC's large rate of W production to study the properties of the W is a worthwhile goal in itself.

This paper examines several of the most important production mechanisms for W at the LHC. These include single W production (Drell-Yan), W produced from $t\bar{t}$ decay, W pair production and WZ production. The relative importance of each production mechanism is analyzed with respect to production rate, usefulness as a signal and difficulties as a background.

Following this introduction is a brief introduction to the Standard Model of particle physics to provide a context for W production. The third section emphasizes the necessity of good W reconstruction for many physical processes at LHC. In the fourth section, four different W production mechanisms at LHC are described in some detail. The final section presents the conclusions of the paper.

2 Standard Model

The Standard Model is the most successful description of particles and their interactions yet developed. It describes matter as being made up of three types of fundamental particles: leptons, quarks and mediators [1]. The leptons and quarks are represented in Table 1.

The model is built on three local gauge symmetries generating the three fundamental forces relevant to particle physics. The three symmetries are the colour, weak and hypercharge symmetries associated with the strong, weak and electromagnetic forces respectively. Each of these forces requires a mediator. The strong force is carried by 8 neutral, massless particles called gluons, while the electromagnetic force is carried by the neutral, massless photon and the weak force is carried by 3 massive particles: the Z^0, W^+ and W^-. These mediators complete the list of known fundamental particles[3] in the Standard Model.

Among the force propagating bosons, the mediators of the weak force ($W^{\pm}$,Z) are unique in that they are very massive. The mass of these particles accounts for the short-range nature of the weak force. The Higgs boson, which is the last remaining undiscovered particle required by the Standard Model, couples to mass and will, if sufficiently massive, decay primarily through W and Z. However, the Higgs boson is not the only heavy standard model particle which will decay primarily through the weak gauge bosons. The top quark decays to Wb pairs virtually 100% of the time. This means that for Standard Model Higgs searches and for top physics studies at LHC it is vital to understand sources of W.

[1] A Toroidal LHC ApparatuS

[2] Compact Muon Solenoid

[3] The Higgs boson is another possible particle for this list, but its existence has not yet been confirmed

	Mass (GeV)	Charge (e)	Family
QUARKS			
d	0.005 to 0.015	-1/3	1
u	0.002 to 0.008	+2/3	1
s	0.100 to 0.300	-1/3	2
c	1.0 to 1.6	+2/3	2
b	4.1 to 4.5	-1/3	3
t	175±6	+2/3	3
LEPTONS			
e	0.0005	-1	1
ν_e	<0.000007	0	1
μ	0.105	-1	2
ν_μ	<0.00017	0	2
τ	1.78	-1	3
ν_τ	<0.00024	0	3

Table 1: The fundamental particles of the Standard Model.

3 Importance of W at LHC

There are several ways to produce W at LHC. Table 2 illustrates the rates of several of these W production mechanisms. This table shows that single W production via Drell-

Process	Cross Section (nb)	Events/Day (L = 10^{34}cm^{-2}s^{-1})
Drell-Yan	209	1.81×10^8
$t\bar{t}$	0.929	8.02×10^5
WW	0.101	8.70×10^4
WZ	3.92×10^{-2}	3.38×10^4
WH M_H = 80 GeV	6.00×10^{-3}	5.18×10^3
H→WW M_H = 600 GeV	1.90×10^{-4}	164

Table 2: Predicted rates of W production at LHC (with K factor of 1.33, see text). WH signal assumes a Higgs mass of 80 GeV, H→WW assumes a Higgs mass of 600 GeV.

Yan is the dominant channel and that the rate of W production at LHC is very high. It also demonstrates that some of the interesting physics channels such as heavy Higgs boson production have rates which are smaller by large factors (eg. 10^6) than other W sources.

This large rate of W production is one of the reasons why understanding W production is important at LHC. Many physics signals of interest at LHC will proceed through W decay. Furthermore, the large rate of W production allows for precise measurement of W properties. Finally, W production can be a background to many important physics searches

at LHC and must be understood. In this section, three aspects of W production will be examined: W as tag for a physics channel of interest; W itself as the signal of interest; and W as a background source for physics channels of interest.

3.1 W as Tag for a Physics Channel of Interest

Many physics channels of interest at LHC involve the production of one or more W bosons. Two of the important Standard Model particles to be studied at LHC are the Higgs boson and the top quark. This section describes the relevance of W physics to these signals.

In Standard Model Higgs searches, there are several different signals to search for. The most promising channel depends strongly on the Higgs mass. For the light Higgs (80 GeV $< M_H <$ 180 GeV) two of the important Higgs production channels are WH production and Ht$\bar{t}$ production. Each of these signals will involve the production of at least one W (t$\bar{t}$ most often decays to 2 W and 2 b quarks). For the heavy Higgs (180 GeV $< M_H <$ 1 TeV), the decay with the largest branching ratio is H$\rightarrow$WW which will occur nearly 70% of the time. This means that W reconstruction is necessary or useful over the entire Higgs mass range attainable at LHC.

When studying top production and decay, an understanding of W sources is vital. The top quark will decay almost exclusively via Wb, so top physics studies in any channel will require W reconstruction.

For these reasons, W reconstruction is necessary in order to reconstruct signals in both Standard Model Higgs and top physics studies at LHC.

3.2 W as Signal

In addition to requiring W reconstruction in order to be sensitive to other physics channels of interest, the reconstruction of W decays can, in itself, provide valuable information about the Standard Model.

Using W production as the signal of interest at LHC can provide measurements of W boson parameters such as its mass. By the time the LHC starts producing collisions for physics, it is expected that LEP II will have been able to measure the mass of the W to within 40 MeV and that Fermilab will have been able to further improve this precision to 35 MeV[2]. It has been estimated[2] that the LHC experiments can be expected to improve this measurement to better than 15 MeV.

In addition to providing information about the W boson itself, W production can be used to test the gauge boson couplings in the Standard Model. W produced with another W or Z boson can provide a test of three-vector boson coupling[3]. These signals can indicate the presence of non-standard physics and provide insight into the structure of the Higgs sector[4].

3.3 W as Background

W boson production is a major source of background to many processes at LHC. As mentioned previously, several important physics channels, including Higgs and top decay, proceed through W. Of course, this means that W production from other sources are major backgrounds to these signals. For example, Table 2 shows that the rates for Drell-Yan, t$\bar{t}$, WZ and WW are large compared to the rate of production of the Higgs signals. In many cases, some form of W production is the single greatest background problem for these signals.

4 W Production Mechanisms

In this section, four different mechanisms for producing W at LHC are presented. The cross section (as calculated in PYTHIA [5]) for each of these processes is shown as a function of centre of mass energy in Figure 1[4]. This figure illustrates the very high rate of W production expected at LHC, estimated at more 2×10^{10} W/year. This plot also shows that the dominant W production mechanism over the entire energy range ($\sim$ 600 GeV $\rightarrow$ 20 TeV) is single W production via the Drell-Yan process.

A large uncertainty in the cross sections shown in this section is the choice of parton density function (pdf) set used in the calculation. To illustrate the problem, consider Figure 2 in which the cross section for the Drell-Yan process is compared for four different pdf sets. The resulting cross sections vary by up to 30% at LHC energy depending on the choice of pdf set. Unless otherwise stated, the pdf set used in this paper is CTEQ2M [6], which is one of the sets currently preferred by the CDF collaboration[5]. The default set in PYTHIA 5.7 [5] is CTEQ2L[6], which is also shown in Figure 2.

It should be noted that these plots show cross sections without applying even level 1 trigger cuts. In reality, at a high luminosity hadron collider such as LHC, certain cuts will always need to be made in order to reduce the data rate to a manageable level and to reduce the data set to a reasonable size. One of the most important cuts of this nature which will be used at LHC detectors is a minimum transverse momentum cut. This type of cut is useful because the vast majority of the physical processes of interest will be hard scattering (high p_T) events. Therefore, a simple p_T cut can be of great value in reducing the background of so-called minimum-bias events. The standard p_T cuts made to reduce minimum-bias background at LHC detectors could potentially influence the relative rates associated with W production. However, in the case of the signals shown in Figures 1 and 2, applying ATLAS level 1 trigger cuts[7] has only a small effect on the relative rates.

4.1 Drell-Yan

The W production mechanism with the highest cross section at LHC is the Drell-Yan process represented by the Feynman diagram in Figure 3.

The cross section for this diagram can be calculated directly. The cross section of the corresponding elementary process is given by:

$$\hat{\sigma}(q\overline{q}' \rightarrow W^+) = 2\pi |V_{qq'}|^2 \frac{G_f}{\sqrt{2}} M_W^2 \delta(\hat{s} - M_W^2). \tag{1}$$

Using the Parton Model one can then obtain

$$\frac{d\sigma}{dy}(W^+) = K \frac{2\pi G_f}{3\sqrt{2}} \sum_{q,\overline{q}'} |V_{qq'}|^2 x_i x_j q(x_i, M_W^2) \overline{q}'(x_j, M_W^2) \tag{2}$$

where y is the rapidity[6] and x_i and x_j are obtained from:

$$x_{i,j} = \frac{M_W}{\sqrt{s}} e^{\pm y}.$$

[4]Each of the curves in this figure are multiplied by a factor of 1.33 to account for 1st order QCD corrections. In reality, a "K factor" of 1.33 is only correct for the Drell-Yan process, for each of the other processes the factor should be slightly different. However, for the purposes of this paper, the same constant has been applied to all signals.

[5]CDF is the Collider Detector at Fermilab, a general-purpose experiment at the Tevatron (currently the world's highest energy collider).

[6]$y = \ln[(E + P_L)/(E - P_L)]$, where P_L refers to longitudinal momentum.

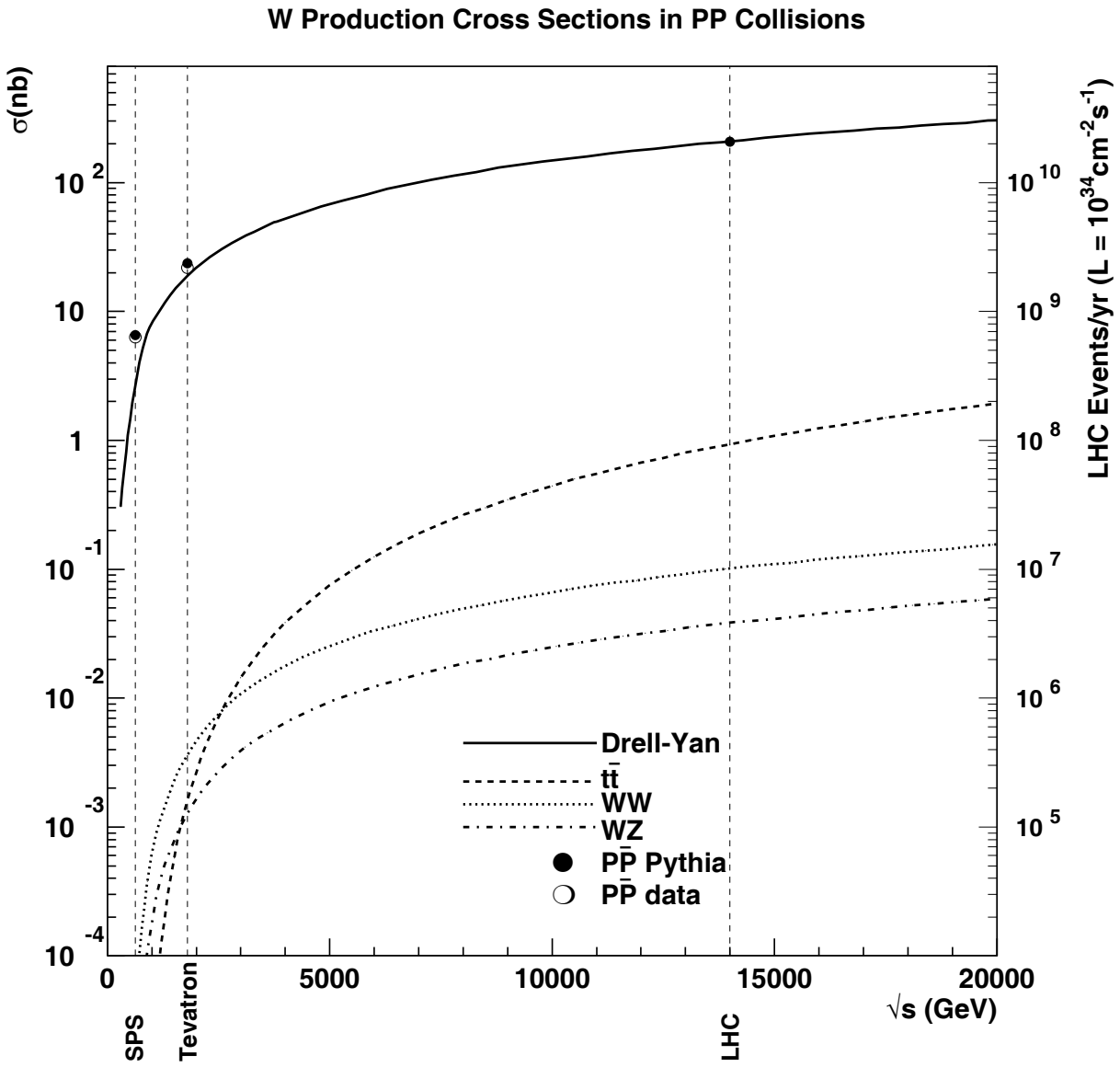

Figure 1: The cross section curves for W production by 4 different processes in pp collisions are shown. Full circles represent the Drell-Yan process for $p\overline{p}$ collisions and empty circles are actual experimental results from $p\overline{p}$ colliders[8][9]. Cross sections were calculated using PYTHIA 5.7 [5], a K-factor correction of 1.33 was applied to the results. Here an LHC year is assumed to be 10^7s.

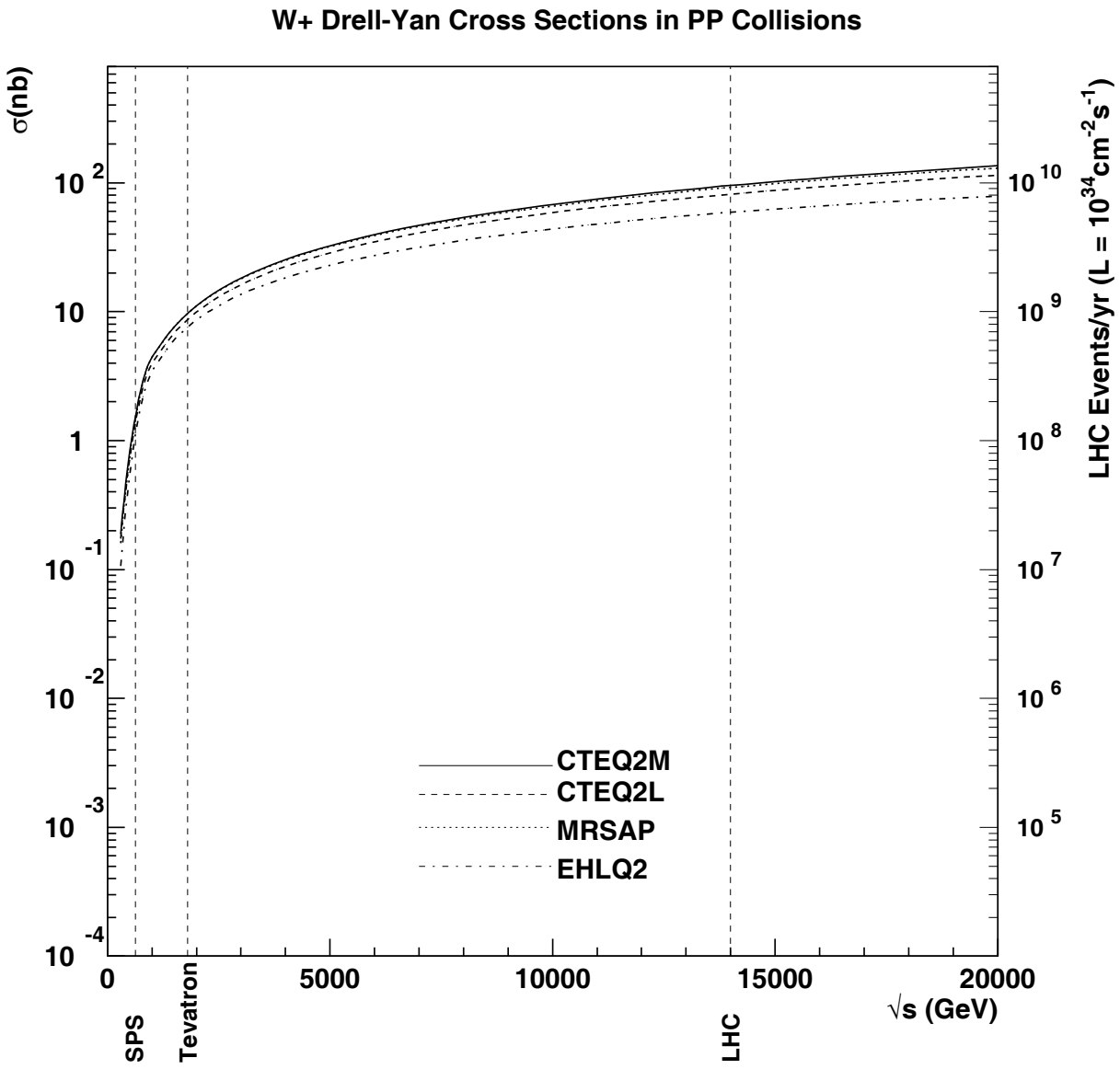

Figure 2: The cross sections for W production by Drell-Yan in pp collisions using 4 different sets of parton density functions.

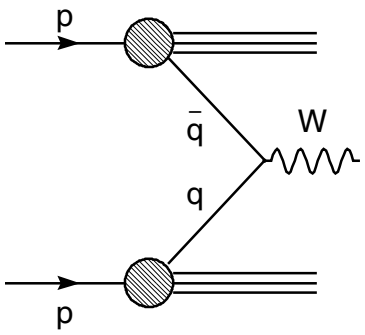

Figure 3: The Feynman diagram for W production via Drell-Yan process at a pp collider.

The final result for the total cross section is obtained by integrating over the kinematically allowed rapidity range (determined by $x_{i,j} \leq 1$)

$$-\ln \frac{\sqrt{s}}{M_w} \leq y \leq \ln \frac{\sqrt{s}}{M_w}.$$

A derivation of these formulae can be found in Appendix A.

Using the above results, the cross section for W^+ production can then be obtained for a given set of parton density functions. Figure 4 shows the cross section curve for W+ from Drell-Yan as produced by Monte Carlo compared to the cross section resulting from the direct calculation above. The curves shown were both produced using the CTEQ2M [6] parton density function set. The agreement between the calculated and Monte Carlo values for the cross section over the entire energy range under study is verified.

The Drell-Yan process has a cross section of 209 nb (using K = 1.33) at 14 TeV centre of mass energy. This means that at high luminosity (10^{34} $cm^{-2}s^{-1}$), 1.8×10^8 W will be produced each day via Drell-Yan. This high rate of production would appear to make this a promising channel for the study of W physics at the LHC. However, since W will decay to 2 jets about 70% of the time, all processes that produce at least 2 jets will be a background for W production via Drell-Yan. The cross section for jet production at LHC is approximately $10^5 - 10^6$ times larger than the cross section for Drell-Yan W production. This means that without a powerful tool for identifying W produced via Drell-Yan, this jet-jet signal will be completely swamped by QCD sources of jets.

Since the Drell-Yan process creates only the W and no other good "tagging" particles, a thorough knowledge of the characteristics of the W and its decay products are the only ways to distinguish the signal from the background. Figure 5 shows that the leptonic decay products of a Drell-Yan W have, on average, a much lower transverse momentum than the decay products from other W sources. These low p_T values mean that these particles will not be easily distinguishable from the "sea" of low p_T jets produced in proton-proton collisions that can fake a lepton signature. Nonetheless, in the case of leptonic W decay this distinction should be made at the LHC experiments and, for this reason, the Drell-Yan W will be reconstructed primarily through its leptonic decays.

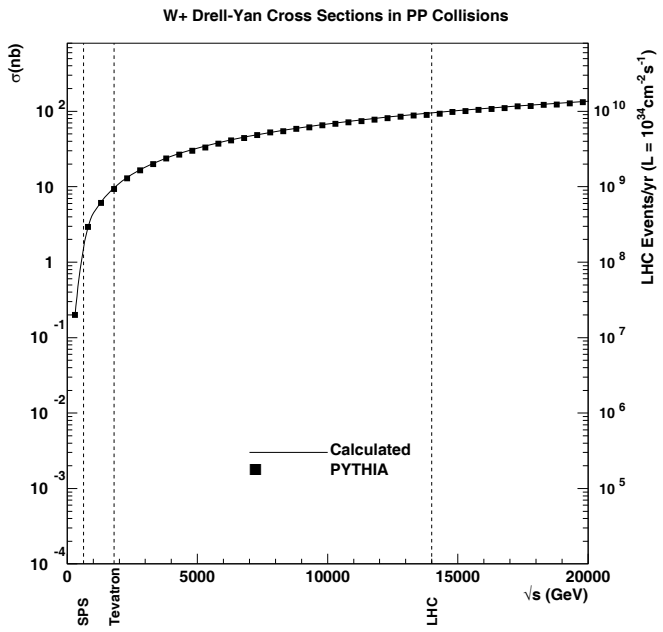

Figure 4: Cross section comparison of PYTHIA and direct calculation.

Figure 6 shows the p_T distribution of the W produced by the Drell-Yan process in relation to W produced by other processes. Though the experiment will directly measure the decay products of the W and not the p_T of the W itself, the p_T of the W is, nonetheless, an interesting quantity. Previous Monte Carlo based studies [10] show that low p_T W are much more difficult to reconstruct from jets than are high p_T W at ATLAS. These studies show that for ATLAS, the mass resolution of low p_T W is 50% worse than for high p_T W. Pileup effects at high luminosity, which worsen at high pseudorapidity and low transverse momentum, make the situation even worse, substantially degrading mass resolution of low p_T W. So, even if it is possible to somehow distinguish these W from their backgrounds, they are not the best candidates for precise measurement of the properties of the W.

Since W from Drell-Yan is difficult to reconstruct in the jet-jet decay mode, only the $l\nu$ channel provides considerable promise for reconstructing W produced by this process. Using this signal, it has been estimated that the W mass can be reconstructed with an uncertainty of less than 15 MeV at LHC[2]. This will then be the best measurement of the W mass available.

4.2 $t\bar{t}$

Another important W production mechanism at the LHC is W production from top decay. The dominant top channel at LHC is $t\bar{t}$ production (represented by the Feynman diagrams of Figure 7) which has a cross section approximately 5 times[11] that of single top production.

LHC is sometimes referred to as a "top factory" due to its large rate of production of top quarks, with a cross section of 0.93 nb (using K = 1.33). This means that at high

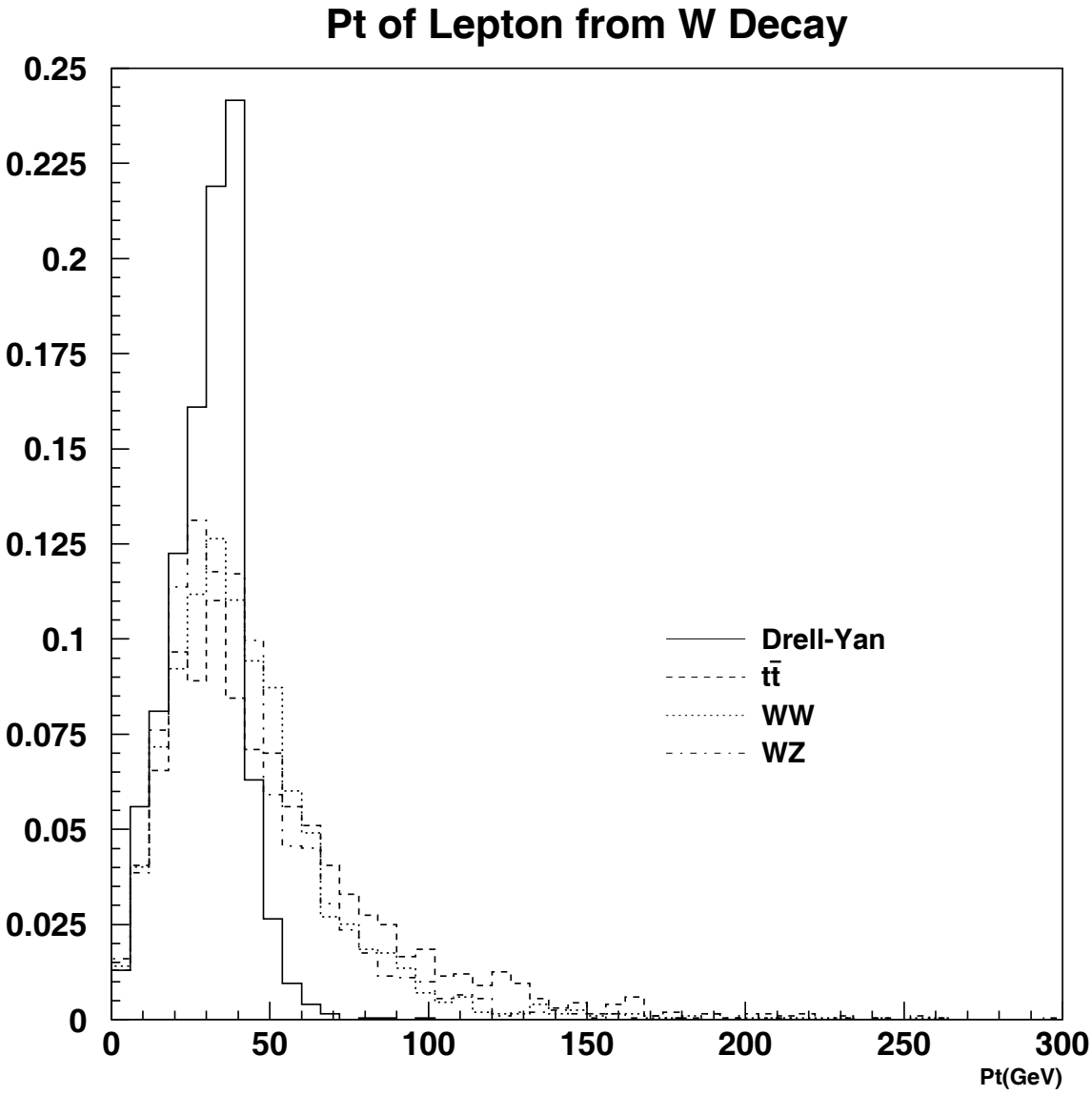

Figure 5: Normalized p_T distributions of the highest p_T lepton from a W for each production mechanism. Calculations were done using PYTHIA 5.7 [5].

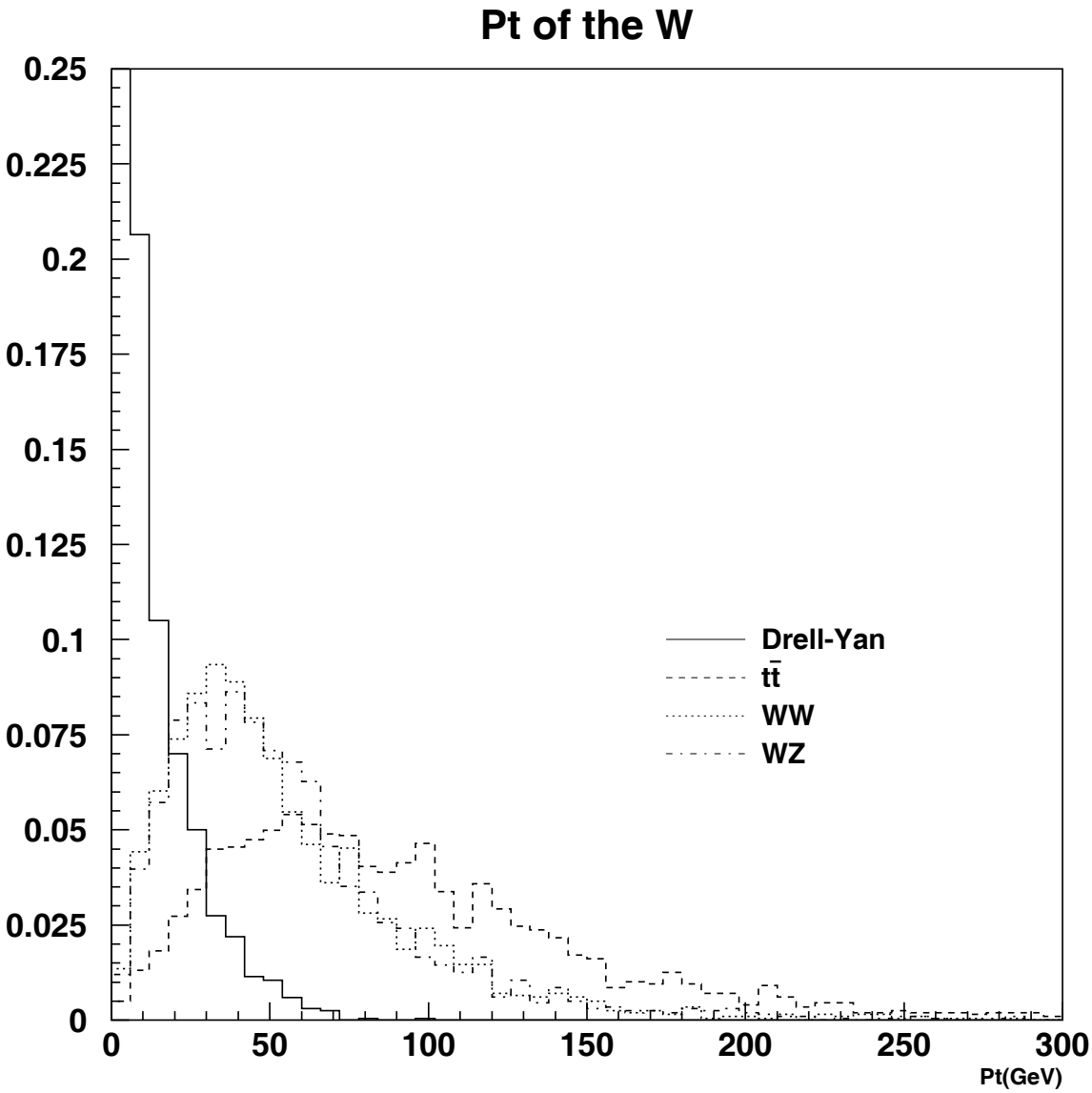

Figure 6: Normalized p_T distribution for W produced via 4 different mechanisms in 14 TeV pp collisions.

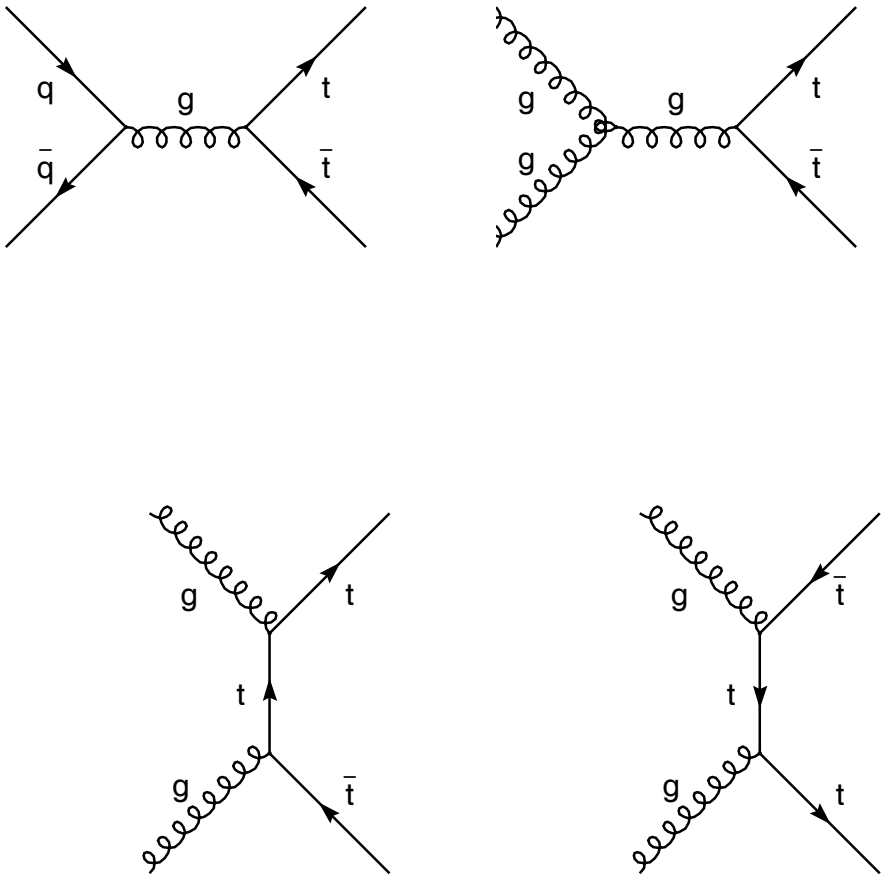

Figure 7: The tree level Feynman diagrams for $t\bar{t}$ production at the LHC.

luminosity (10^{34}cm^{-2}s^{-1}), 8×10^5 $t\bar{t}$ pairs will be produced each day. Since top decays to Wb virtually 100% of the time, an equal number of W pairs from $t\bar{t}$ decay will be produced daily. This high rate of production leads to two important conclusions: 1) understanding sources of W at LHC is essential for doing top physics; 2) $t\bar{t}$ is a major source of high p_T W at LHC, making it a serious background to many physics processes expected to proceed through W decay.

There are several factors which make reconstruction of W produced via $t\bar{t}$ more promising than W produced via Drell-Yan. Most importantly, there are now powerful constraints which were not present in the Drell-Yan signal, such as the top mass and the fact that there are two W in the event. Since the mass of the top is already known to 3.4%, its value can be used to identify Wb pairs that come from top decay. Another constraint on W from $t\bar{t}$ is the presence of two b-quark jets in every event. If one or both of these b-jets can be tagged, backgrounds to this signal could then be reduced.

Even without these new constraints based on the particle content of the events, $t\bar{t}$ has advantages over Drell-Yan. From Figure 5, we see that leptons from the decay of W produced via $t\bar{t}$ have a harder p_T distribution than that of Drell-Yan. Leptons from a W produced via $t\bar{t}$ have a greater chance of being distinguishable from the low p_T minimum-bias background at LHC due to the significant high-p_T content in the $t\bar{t}$ distribution.

Once it has been determined that the reconstructed event contains a W there is another issue to consider. That is, how well it is possible to reconstruct the mass of the W from this signal. In the previous section, reference was made to the fact that it has been shown previously [10] that, in general, better mass resolution has been obtained from the reconstruction of the decay of high p_T W than of low p_T W. Figure 6 shows that of all of the W production mechanisms considered here, $t\bar{t}$ has the largest fraction of events with a high p_T W.

From these considerations, it appears that $t\bar{t}$ is a promising channel for reconstructing and studying W at LHC. However, the importance of $t\bar{t}$ as a W source is not limited to the study of the W itself. Since it will be one of the most well defined W signals at LHC and because it is produced at such a high rate, it is a good candidate to be used for in-situ calibration of the calorimetry of ATLAS and CMS. As well, because of its high rate and the high p_T W produced, $t\bar{t}$ is a major source of background for several important physics channels, including H$\rightarrow$WW.

4.3 W Pair

The third important W production mechanism considered here is W pair production (represented by the Feynman diagrams of Figure 8). This process has a cross section of 0.10 nb (assuming K=1.33) at 14 TeV centre of mass energy. This means that at high luminosity (10^{34} cm^{-2}s^{-1}), 87000 W pairs will be produced each day via WW.

In the Standard Model there are important cancelations in the amplitudes for W^+W^- and $W^{\pm}Z^0$ production which rely on the gauge structure of the WWZ trilinear coupling [12]. Looking at Figure 8, one can see that there will be contributions to the cross section for this process from γ, Z and quark exchange. This means that this cross section is particularly sensitive to the interplay among the different gauge boson contributions. It is important to verify that the amplitude for this process behaves as expected [12] and that these cancelations occur. At LHC, with 100 fb^{-1} it will be possible to place limits on anomalous WWV and ZγV couplings which are a factor of 3 to 100 better than one can expect with the Tevatron or LEP II[13].

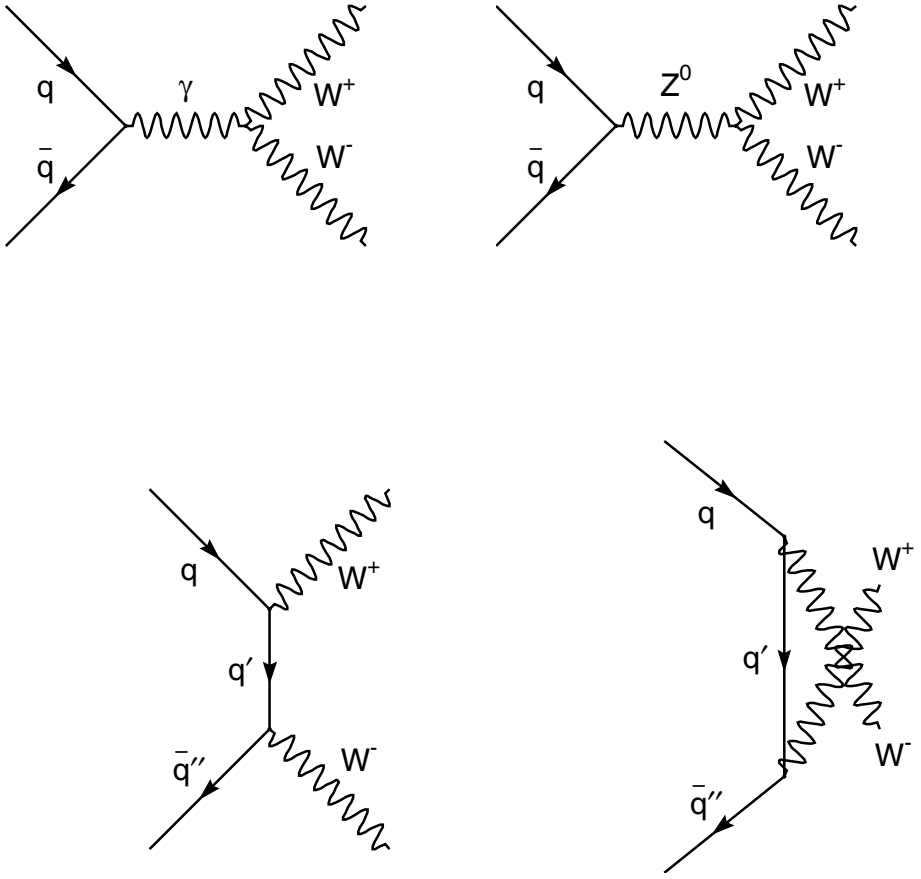

Figure 8: The tree level Feynman diagrams for W pair production at a pp collider. The bottom two diagrams represent similar processes with a u-type incoming q (on the left diagram) and a d-type incoming q (on the right diagram).

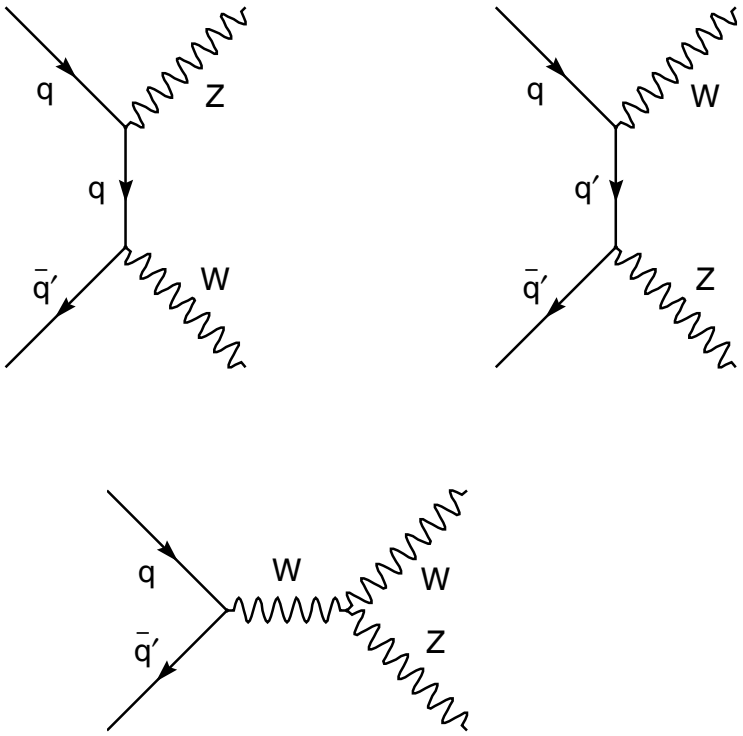

Figure 9: The tree level Feynman diagrams for WZ production at a pp collider

In order to test the electroweak couplings, it is, of course, necessary to be able to distinguish this WW signal from its backgrounds. One of the major sources of background to the WW signal is the $t\bar{t}$ production described in the preceding section. There are, of course, extra constraints in the $t\bar{t}$ signal, chief among them the top mass and the presence of a pair of b jets. These constraints should be very helpful in obtaining a sample of WW events. The p_T distribution of leptons, shown in Figure 5, is helpful in reducing background from low p_T minimum bias events, but is very similar for WW and $t\bar{t}$ and so would not, in itself, be a very powerful tool in distinguishing the two signals.

4.4 WZ

The final LHC W production mechanism treated in this paper is WZ production, represented by the Feynman diagrams of Figure 9. This process has a cross section of 0.039 nb (assuming K=1.33) at 14 TeV centre of mass energy. This means that at high luminosity (10^{34} $cm^{-2}s^{-1}$) 34000 W will be produced each day via WZ.

As for the WW case, the WZ signal is useful for probing the gauge structure of the

electroweak interactions[12]. It is also a source of background for Higgs searches at LHC. In particular, WZ is considered a serious background source to light Higgs ($80 < M_H < 120$ GeV) searches in the WH channel[3] and is one of the backgrounds for heavy Higgs (180 GeV $< M_H <$ 1 TeV) in the H$\rightarrow$ZZ$\rightarrow$ $ll\nu\overline{\nu}$ channel. If the Higgs has a mass greater than 1 TeV, it becomes strongly interacting and in this mass regime WZ is once again a background source. So, WZ is a Higgs background in some channel over the entire Higgs mass range available to the LHC.

5 Conclusions

The rate of W production at LHC will be more than 1.8×10^8 per day per experiment at full luminosity. W production is therefore an important component of the physics programme at ATLAS and CMS. Most of these W are produced singly via the Drell-Yan process. However, $t\overline{t}$, WW and WZ production each produce large quantities of W and can also be important. In particular, $t\overline{t}$ is considered the best signal for measuring top mass at LHC and, because it is a source of high p_T W, it is also a background to physics channels of interest. Vector boson pair production (WW or WZ) provides an excellent opportunity to measure the Standard Model couplings for the three-boson vertex, and can also act as a background to top reconstruction and Higgs searches. The high rate will also allow properties of the W, such as its mass, to be measured to better precision than existing experiments.

References

[1] Griffiths, David, J., *Introduction to Elementary Particles*, John Wiley and Sons, New York, 1987.

[2] Keller, S. and Womersley, J., Measuring the Mass of the W at LHC, *To appear in the proceedings of the 1996 DPF/DPB Summer Study on New Directions for High-Energy Physics (Snowmass 96), Fermilab-Conf-96/422-T*, November 1996.

[3] Armstrong, W. et al. (ATLAS Collaboration), Technical Proposal for a General-Purpose pp Experiment at the Large Hadron Collider at CERN, *CERN Internal Publication*, CERN/LHCC/94-43, December 15, 1994.

[4] Fouchez, D., Gauge bosons pairs production study with ATLAS, *ATLAS Internal Note, PHYS-NO-060*, November 24, 1994.

[5] Sjöstrand, T., Computer Physics Communications 82 (1994) 74.

[6] Botts, J. et al., Phys. Lett. B304 (1993) 159

[7] Bystricky, J. et al., ATLAS trigger Menus at Luminosity $10^{33}\mathrm{cm}^{-2}\mathrm{s}^{-1}$, *ATLAS Internal Note, DAQ-NO-054*, June 17, 1996.

[8] Alitti, J. et al. (UA2 collaboration), A Measurement of the W and Z Production Cross Sections and a Determination of Γ_W at the CERN $\mathrm{p\overline{p}}$ Collider, *Physics Letters B*, 276 (1992) 365-374, October 7, 1991.

[9] Grudberg, P.M., Measurement of the W and Z Boson Production Cross Section in $\mathrm{p\overline{p}}$ Collisions at $\sqrt{s}$ = 1.8 TeV with the D0 Detector, *Phd Thesis, University of California at Berkley*, Spring 1997.

[10] Savard, P., The W→jet-jet and Top Mass Reconstructions with the ATLAS Detector,*ATLAS Internal Note CAL-NO-092*, May 6, 1997.

[11] Ferbel, T., More on Single Top-Quark Production at ATLAS, *ATLAS Internal Note, PHYS-NO-069*, July 31, 1995.

[12] Eichten, E. et al., Supercollider Physics, *Reviews of Modern Physics*, Vol. 56, No. 4, October 1984.

[13] Amidei, D. and Brock, R., Future Electro Weak Physics at the Fermilab Tevatron: Report of the tev_2000 Study Group, *Fermilab-Pub-96-082*, April 1, 1996.

A Drell-Yan Cross Section Calculation

First calculate the cross section for the elementary process $q_i\overline{q}_j \to W^+$ using the Feynman rules. The matrix element is given by

$$\mathcal{M} = \underbrace{\overline{v}(i)}_{q_i} \overbrace{\frac{-ig_w}{2\sqrt{2}}\gamma^\mu(1-\gamma^5)V_{ij}}^{\text{vertex}} \underbrace{u(j)}_{q_j} \overbrace{\epsilon^*_\mu}^{W},$$

squaring we get

$$|\mathcal{M}|^2 = |V_{ij}|^2\frac{g^2}{8}\left(\epsilon^*_\mu\overline{v}(i)\gamma^\mu(1-\gamma^5)u(j)\right)\left(\epsilon^*_\nu\overline{v}(i)\gamma^\nu(1-\gamma^5)u(j)\right)^*,$$

Summing over final states and averaging over initial states introduces a factor of $1/3$ due to colour and $1/4$ due to the average over initial spins. The summing is done over all spin and polarisation states.

$$\overline{|\mathcal{M}|^2} = \left(\frac{1}{3}\right)\left(\frac{1}{4}\right)\sum_{spins}\sum_{pol}|\mathcal{M}|^2$$

Evaluating the sum over spins using Casimir's Trick gives

$$\sum_{spins}|\mathcal{M}|^2 = |V_{ij}|^2\frac{g^2}{8}\epsilon^*_\mu\epsilon_\nu\left[2Tr(\gamma^\mu \not{p}_j \gamma^\nu \not{p}_i) + 8i\epsilon^{\mu\alpha\nu\beta}p_{j\alpha}p_{i\beta}\right].$$

Evaluating the trace, we find

$$\sum_{spins}|\mathcal{M}|^2 = |V_{ij}|^2\frac{g^2\epsilon^*_\mu\epsilon^*_\nu}{8}\left[2\times 4(p_j^\mu p_i^\nu + p_j^\nu p_i^\mu - (p_i\cdot p_j)g^{\mu\nu}) + 8i\epsilon^{\mu\alpha\nu\beta}p_{j\alpha}p_{i\beta}\right].$$

Evaluating the sum over W polarisations

$$\sum_{\lambda=1}^{3}\epsilon^\lambda_\mu\epsilon^\lambda_\nu = -g_{\mu\nu} + \frac{p_\mu p_\nu}{M_w^2}$$

$\epsilon^{\mu\alpha\nu\beta}$ is a totally anti-symmetric symbol whereas the sum over polarisations shown above gives a symmetric result. Therefore, terms in $|\mathcal{M}|^2$ containing $\epsilon^{\mu\alpha\nu\beta}$ will not contribute to the final result and can be discarded.
Therefore,

$$\overline{|\mathcal{M}|^2} = \frac{|V_{ij}|^2g^2}{4\cdot 3}(p_j^\mu p_i^\nu + p_j^\nu p_i^\mu - (p_i\cdot p_j)g^{\mu\nu})(-g_{\mu\nu} + \frac{p_\mu p_\nu}{M_w^2})$$

Multiplying and using $g^{\mu\nu}g_{\mu\nu} = 4$ we obtain

$$\overline{|\mathcal{M}|^2} = \frac{|V_{ij}|^2g^2}{4\cdot 3}\left[2p_j\cdot p_i + \frac{2(p\cdot p_j)(p\cdot p_i)}{M_w^2} - (p_j\cdot p_i)\frac{p\cdot p}{M_w^2}\right].$$

Next, using $p\cdot p = M_w^2$ we get

$$\overline{|\mathcal{M}|^2} = \frac{|V_{ij}|^2g^2}{4\cdot 3}\left[p_j\cdot p_i + \frac{2(p\cdot p_j)(p\cdot p_i)}{M_w^2}\right]. \tag{3}$$

Choose centre of mass system

First, find $\mathrm{p}_j \cdot \mathrm{p}_i$:

$$p_i = (E_i, 0, 0, p_{iz})$$

$$p_j = (E_j, 0, 0, -p_{iz})$$

$$p = p_{\mathrm{W}} = p_i + p_j = (E_i + E_j, 0, 0, 0)$$

$$E_i^2 = |p_i|^2 + m_i^2, \qquad \text{neglect quark masses} \Rightarrow m_i^2 = 0$$

$$\text{so, } E_i^2 = |p_i|^2$$

$$p_j \cdot p_i = E_i E_j + p_{iz}^2 = p_{iz}^2 + p_{iz}^2$$

$$p_j \cdot p_i = 2p_{iz}^2. \tag{4}$$

Next, find $(\mathrm{p}\cdot\mathrm{p}_j)(\mathrm{p}\cdot\mathrm{p}_i)$ where p refers to the momentum of the W:

$$p \cdot p_j = (E_i + E_j)E_j$$

$$p \cdot p_i = (E_i + E_j)E_i$$

$$(p \cdot p_j)(p \cdot p_i) = (\underbrace{E_i + E_j}_{E_w})^2 E_i E_j$$

$$E_w^2 = M_w^2 \qquad \text{W produced at rest in this frame, } |\vec{p}| = 0$$

$$E_w = M_w = 2p_{iz} \qquad \text{since } E_i = p_{iz} = E_j$$

so,

$$\begin{aligned}(p \cdot p_j)(p \cdot p_i) &= M_w^2 E_i E_j \\ &= M_w^2 p_{iz}^2 \\ &= M_w^2 \tfrac{M_w^2}{4} \\ (p \cdot p_j)(p \cdot p_i) &= \tfrac{M_w^4}{4}. \end{aligned} \tag{5}$$

Substituting equations 4 and 5 into 3 gives

$$\overline{|\mathcal{M}|^2} = \frac{|V_{ij}|^2 g^2}{4 \cdot 3}\left[\frac{M_w^2}{2} + \frac{M_w^2}{2}\right]$$

$$\overline{|\mathcal{M}|^2} = \frac{|V_{ij}|^2 g^2 M_w^2}{4 \cdot 3}. \tag{6}$$

In order to calculate the cross section from this matrix element, use the Golden Rule for n final state particles:

$$d\sigma = \frac{1}{2\lambda^{\frac{1}{2}}(s, m_a^2, m_b^2)(2\pi)^{3n-4}} \sum \overline{|\mathcal{M}|^2} \delta^4(p_a + p_b - \sum_{i=1}^{n} p_i) \prod_{i=1}^{n} \frac{d^3 p_i}{(2E)_i}$$

where

$$\lambda(x,y,z) = x^2 + y^2 + z^2 - 2xy - 2xz - 2yz.$$

In this case n=1, m_a =m_b = 0. Using this gives

$$d\sigma = \frac{1}{2(s)(2\pi)^{-1}} \overline{|\mathcal{M}|^2} \delta^4(p_a + p_b - p) \frac{d^3p}{(2E)_w}. \tag{7}$$

Evaluating the phase space gives

$$\int \frac{d^3p}{2E_w} \delta^4(p_a + p_b - p) = \delta(s - M_w^2).$$

Substituting, we get

$$\begin{aligned} \sigma &= \frac{\pi}{s} \overline{|\mathcal{M}|^2} \delta(s - M_w^2) \\ &= \frac{\pi}{s} \delta(s - M_w^2) \left[\frac{|V_{ij}|^2 g^2 M_w^2}{4 \cdot 3} \right]. \end{aligned}$$

Using

$$g^2 = \frac{8}{\sqrt{2}} G_f M_w^2 \text{ and } s = M_w^2$$

we obtain

$$\sigma(qq \rightarrow W^+) = \frac{2\pi}{3} |V_{ij}|^2 \frac{G_f}{\sqrt{2}} M_w^2 \delta(s - M_w^2). \tag{8}$$

Now that we have found the cross section for the elementary process qq$\rightarrow$ W^+, we can use the parton model to get the cross section for the corresponding process pp$\rightarrow$ W^+. The parton model yields

$$\sigma(pp \rightarrow W^+) = \int dx_i \int dx_j \sum_q q(x_i) \overline{q'}(x_j) \hat{\sigma}$$

where $\hat{\sigma}$ is the cross section of the corresponding elementary process and

$$\begin{aligned} \hat{s} &= x_i x_j s; \\ \sqrt{\hat{s}} &= \text{invariant mass of the quark system;} \\ \sqrt{s} &= \text{invariant mass of the proton system;} \\ x_i &= \text{momentum fraction of } q_i \text{ in } P_i; \\ x_j &= \text{momentum fraction of } q_j \text{ in } P_j; \\ q(x_i) &= \text{parton density function for interacting quark;} \\ \overline{q'}(x_j) &= \text{parton density function for interacting antiquark;} \\ y &= \text{rapidity, defined as } \frac{1}{2} \ln \frac{x_i}{x_j}. \end{aligned}$$

In order to ensure that the integrals are well suited for numerical evaluation (ie. no sharp peaks in the integrand) we transform the integration to $\hat{s}$ and rapidity (y) variables using the following transformation

$$dx_i dx_j = \frac{d\hat{s} dy}{s}$$

The delta function disappears in the integral over $\hat{s}$ leaving

$$\frac{d\sigma}{dy}(W^+) = \frac{2\pi G_f}{3\sqrt{2}} \sum_{q,\overline{q'}} |V_{q,q'}|^2 x_i x_j q(x_i)\overline{q'}(x_j), \tag{9}$$

where x_i and x_j are evaluated at

$$x_{i,j} = \frac{M_w^2}{\sqrt{s}} e^{\pm y}.$$

The final result for the total cross section is obtained by integrating over the allowed rapidity range (determined by $x_{i,j} \leq 1$)

$$-\ln \frac{\sqrt{s}}{M_w} \leq y \leq \ln \frac{\sqrt{s}}{M_w}.$$